arXiv:astro-ph/9411039v1 10 Nov 1994

PUPT-xxxx

Angular Momentum and Large-Scale Magnetic Field in Textures Seeded Models

Hugues Sicotte[†]

Joseph Henry Laboratories
Princeton University
Princeton, New Jersey 08544
sicotte@pupgg.princeton.edu

Abstract

We start by reviewing the problem of large scale magnetic fields. We explain the acquisition of angular momentum in the general context of Dark Matter models and we use this result to derive a dynamical mechanism for magnetic field generation. This mechanism does not produce any magnetic field for standard CDM, but it does for a large class of other models. We apply this mechanism in the context of the texture scenario of large-scale structure formation. Resulting constraints on the texture scenario and other models are discussed.

November 1994

[†] work supported in part by NSF

1. Introduction

There is strong observational evidence for a large scale galactic magnetic field in our galaxy and in neighbouring galaxies . From the early polarisation of starlight measurements [1][2] to the more recent observations of the faraday rotation of pulsar emissions or other extra-galactic sources, there is a strong experimental evidence of such field. The galactic magnetic field is also required to explain why cosmic ray composition makes it appear that they have been through 30 to 300 time as much matter as there is between us and the galactic center. Alfvén and Fermi (1949) first discussed this and predicted a field of 10μgauss to confine the cosmic rays in the galactic plane, this is very close to the current $2-3\mu$gauss value for the coherent component. Current theories of this magnetic field creation require a seed field which is then amplified by a dynamo mechanism. [3]

In addition, more recent observations show that there seem to be a magnetic field on cluster size. Any theory of large scale structure should predict some seed magnetic field uniform on a galactic scale, the texture mechanism [4]does this in a very natural fashion.

The outline of this paper is as follow. In section 2, we will describe how one generically generates magnetic field with a model of cosmological perturbations. In section 3, we will briefly describe the model of large scale structure formation by textures, and quote some of the results we will be using. In section 4 we will apply the formalism of section 2 to the texture model of structure formation and calculate the magnetic field it generates. In section 5 we will discuss the results and the implications for texture and compare to other candidate model of structure formation.

1.1. Notation

When discussing physics happening around matter-radiation equality, it is natural to refer scales to that era, so we will use a scale factor normalised at matter-radiation equality: $a(t), \text{where} a(t_{eq}) \equiv 1$. Sometimes we will use the more common scale factor defined as $\frac{R}{R_0} \equiv \frac{1}{(1+z)}$. Spatial distances denoted by x , will always be in co-moving coordinates in units of Mpc. x_{eq} denotes co-moving coordinates with a value that they would have at Matter-Radiation equality, x without the eq subscript denotes the normal co-moving coordinates, referenced to the present time. k will denote $\frac{2\pi}{\lambda}$ and will be in co-moving units of Mpc^{-1}; here again k_{eq} will be referenced to equality, and k without a subscript will be referenced to the present.

Time for a co-moving observer ,t, will be given in units of ls . Where 1 ls$= 2\sqrt{2}c\tau_* \approx 2.79 \times 10^{12}$ seconds We will convert between a and t using

$$t = \frac{t_{eq}}{2-\sqrt{2}}\left((1+a)^{\frac{3}{2}} - 3\sqrt{1+a} + 2\right) \tag{1.1}$$

and it's numerical inverse. Variables with a subscript i (i.e. a_i , τ_i) refer to the value of that variable at the epoch when a given texture just collapsed.

1.2. CDM Model

In all following discussions standard CDM will refer to a Cosmology with a scale invariant Harrison-Zeldovich (HZ) spectrum. For both CDM and the Texture model we will use a model with critical density $\Omega = 1$, with a Dark Matter component $\Omega \sim 0.95$ and a baryonic fraction of 5% . For the standard CDM model, we will assume a Hubble constant of $50km/s/Mpc$, while for the textures model we will assume a Hubble constant of $75km/s/Mpc$. For our purposes, the exact composition of the model makes little difference as long as most of the matter is Dark Matter.

Throughout this article we will use DM when speaking about the dark matter, while baryonic and leptonic matter and photons will be refered to as matter.

2. Magnetic Field Generation

When thinking about magnetic field generation, it is useful to separate the physics in 2 phases. First a seed field, B_{seed}, is created before a galaxy collapses. In the second phase the magnetic field is first amplified by flux conservation during collapse and then by a dynamo process.

The seed field creation ceases after the protons and electrons present in the primordial plasma recombine. The flux lines are then frozen in the interstellar gas due to the large conductivity of the plasma.

For an introduction to the dynamo theory see [5][6][7][8]. The dynamo amplification mechanism occurs in galactic objects. The flux is amplified through processes that makes flux lines buckle and form loops arcing above the galactic plane . These loops twist 180°, rejoin and fall back on the galactic plane, increasing the flux line density. For example, a cloud of gas can rise due to buoyancy forces, it then expands due to the lower density of gas above the galactic plane. As it expands, the coriolis force makes the cloud rotate, twisting

the lines of flux as they are frozen in the cloud. The cloud then cools and falls back onto the galactic plane, carrying the loop back in the plane. This process increases the random field, B_{rms}. The ensemble average of these random fields has a growing coherent mode. It is a topic of some controversy as to whether this yields an exponential or a linear increase of the magnetic field [9][10][11].

To get the current value of 3μgauss,with exponential dynamo , seed field values of only about 10^{-18} to 10^{-16}gauss are required at the time of galaxy formation. On the other hand a linear dynamo requires fields of at least $10^{-12}\mu$gauss which are very hard to generate without delicate adjustement of large-scale structure generating models. For such an example in the inflationary scenario see [12]

The creation of a seed field of even 10^{-18} gauss is a non-trivial test for a theory to pass. Generically seed field creation can happen in 4 possibles eras. The first one is if the magnetic field has a primordial origin, for example [12]. The next two other eras involve dynamical phenomenas. The last period happens once the structure formation is well advanced. It involves magnetic field expulsed from powerful beamed radio sources.[13]

We will not deal here with theories postulating a primordial of the magnetic field or those postulating the existence of powerful radio sources at very high redshift.

2.1. Harrison scenario

The second era for magnetic field generation is between matter-radiation equality and recombination. If we assume that there was some primordial vorticity, such as could happen in chaotic Cosmology, we can generate magnetic fields using to the following mechanism due to Harrison [14][15].

During that era the electrons motion is tied to that of the photons though the large thompson cross-section, σ_e^T. For the protons ,the proton's thompson cross section, σ_p^T, is much less important than the hadronique neutron-proton cross section. As a result while the electrons move with the photon fluid, the protons together with the neutrons can have a different behavior.

Implicit in the derivation of the Harrison mechanism is the existence of primordial vortices. We can nevertheless define a local scale factor r within the framework of the Homogeneous world model. The eddy follows the expansion and ρr^3 and ρr^4 remain constant for matter and radiation respectively. So the angular momenta of the matter, $\rho\omega r^5$, and the angular momenta of the radiation, $\rho_r\omega_r r^5$, are separately conserved. Therefore $\omega_p \propto \frac{1}{r^2}$ and $\omega_\gamma \sim \omega_e \propto \frac{1}{r}$. This means that electrons and protons will have different

angular velocities, leading to an angular electric field and therefore a poloïdal magnetic field. The value of this field will get frozen in at recombination.

The detailled kinematical analysis can be found in Appendix 1. The final result is

$$B_{recombination} = \frac{-2m_p}{e}\mathbf{w}(z_r) = (-7.4610^{-17} gauss(bs))\mathbf{w}(z_r)(bs)^{-1} \tag{2.1}$$

In an expanding Universe, the initial vorticity ($\zeta = \nabla \times \vec{v}$) perturbations decay as

$$\zeta(a) \sim \frac{1}{a^2} \tag{2.2}$$

.

This mean initial vorticity is washed away unless the universe was very chaotic when it started. Limits on the amplitude of primordial density perturbations by the COBE satellite rule out this possibility unless the universe was re-ionized.

2.2. Harrison-like scenario

The above Harrison scenario fails to pass the experimental tests because it depends on primordial vorticity. We will ressucite the Harrison mechanism, but rely on dynamically generated vorticity. This will yield the third period when magnetic field can be generated. The vorticity in the matter will be generated when the DM collapses early and acquires non-spherical components through tidal torquing. The acoustic waves in the matter, that form as the super-horizon density modes enter the horizon, will then undergo oblique shocks because they are falling in a non-spherical rotating potential. This mechanism will thus create the required vorticity in the matter.

In most theories of Large Scale Structure (LSS) formation the Jeans mass before decoupling is larger than the mass within the Horizon. This is due to the photon pressure which keeps density perturbations initially at rest from growing .

But LSS theories with topological defects generate density perturbations and velocity until very late times, unlike standard LSS scenarios which have all their density perturbation as initial conditions.

In the texture model the density perturbations are not fixed as initial condition. The density perturbation are dynamically generated because of the texture collapse. We will see later that the regions around the center of a collapsing texture get a velocity kick toward that center. The radial component can be approximated by

$$\vec{\mathrm{v}} = \epsilon c\big(1 - \frac{\mathrm{r}}{ct_i}\big) \tag{2.3}$$

where r is the real radius, t_i is the collapse time of the texture and ϵ is the only parameter of the theory and is normalised to COBE. This radial kick allows a texture seeded velocity kick to grow density even though the matter contained within it is lower than the Jeans mass before decoupling.

The velocity kick is calculated for an ideal spherically symmetric texture collapse. Numerical textures simulations show that most textures are not perfectly symmetric and that a small azimuthal velocity is also imparted to the matter surrounding the texture. Typically there are non-radial components to the velocity of approximatively 1 -2 % of (2.3). This is not to say that a vorticity is created, it is a perturbation from a purely radial velocity kick due to the assymetric nature of real textures.

We will not be using the small rms azimutal velocity from the initial collapse for our final result. Instead the initial assymetries in the dark matter, inside the volume of the texture, will be caused by the previous collapse of the smaller textures that were contained in that volume. We will see in section 4 how those assymetries cause the DM halo to gain angular momentum through tidal torques from neighbouring DM halos. We will see how this rotating DM halo will then transfer angular momentum to the matter before the recombination era. This allows some magnetic field generation for late textures by a mechanism similar to the Harrison scenario.

3. Large-scale structure texture seeds

The theory of topological defects as source of large scale structure was first treated by Kibble [16], later Turok [4]showed that global texture could occur naturally in GUT theories and produce interesting density perturbations in the early universe. (See [17][18]for review)

An SU(2) symmetry seems most natural in term of a particle physics model. With a complex higgs field we could have a global SU(2) symmetry . For computational purposes it is easier to deal with a SO(4) 4-component isovector with real fields, so let us consider a GUT theory with a global SO(4) symmetry .

$$\mathcal{L} = \frac{1}{2}\big(\partial_\mu \vec{\Phi}\big)\big(\partial^\mu \vec{\Phi}\big) - \frac{\lambda}{4}(\vec{\Phi}^2 - \Phi_0^2)^2 \tag{3.1}$$

with

$$\vec{\Phi} = \frac{1}{\sqrt{2}} \begin{pmatrix} \Phi_1 \\ \Phi_2 \\ \Phi_3 \\ \Phi_4 \end{pmatrix} \tag{3.2}$$

where the lagrangian is invariant under the global symmetry transformation $\vec{\Phi} \rightarrow \exp \imath\alpha\vec{\Phi}$ with α a constant. In the ground state , $\vec{\Phi}$ develops an expectation value, $< 0|\vec{\Phi}|0 > = (\Phi_0, 0, 0, 0)$, which breaks the symmetry of the lagrangian. . The 1-direction is arbitrary so that, early in the universe, fields not in causal contact will point in different directions. As their event horizon grows and they come in causal contact they may form a field configuration known as texture. This large size field configuration is unstable by derrick's theorem. [19][20] which states that no static soliton solution exists in 3 or more dimensions. So the energy stored in the gradients of the field configuration collapses to the center. At that point the energy density is such as to allow the texture field configuration to topogically unwind over the potential. This leaves the field aligned within the current horizon volume. As the horizon grows, other texture field configurations may appear and collapse. Each time a texture collapses, the energy of the field configuration produces a gravitational attraction toward the center of the texture. The resulting radial velocity kick can be described as

$$\vec{\mathrm{v}} = \epsilon c\big(1 - \frac{\mathrm{r}}{ct_i}\big) \tag{3.3}$$

where $\epsilon = 8\pi G\Phi_\circ^2$ is normalised to COBE. There is a resulting azimutal velocity kick of at most 1-2% of this. The resulting velocity field does not have a net vorticity. This aximuthal component is simply due to the field configuration not being uniformly spherical.

3.1. Power spectrum

In [21] Pen et al.. calculated numerically the power spectrum caused by texture as it would look today. They give a fitting function

$$\frac{VP_{fit}(k)}{(2\pi)^3} = \frac{890(Mpc^4)k}{(1 + 14. \times k + 11 \times k^{1.5})^2} \tag{3.4}$$

We can use the fitted function of the numerical results in [21]and evolve it backwards in time using linear theory and an time dependant cut-off for small k

$$VP(k_{comov}, a) = VP(k_{comoving}) \times \frac{D(a)^2}{D(a_{now})^2} \tag{3.5}$$

where $k_{comov} < \frac{2\pi a}{a_{now}ct}$ and $D(a) = (1 + \frac{3a}{2})$ is the growing mode solution of a density perturbation valid in both the matter and radiation era. [22].

4. Magnetic field by texture

As we saw in section 2, we have to separate the problem of magnetic field generation in 2 phases. In the first phase the texture provided the initial aspherical density perturbation. In the second phase angular momemtum will be provided by torquing by gravitational forces. Note that this process can be also applied to standard CDM.

4.1. Angular Momentum

Once the Texture collapse has seeded a velocity kick in the DM particles, our mechanism still require that the resulting particle distribution acquires a non-spherical distribution. This rotation of the non-symmetric gravitational potential will be acquired through the tidal torquing picture. While in standard CDM the Dark matter cannot collapse this early, the tidal torquing picture of Peebles [22]can still be applied. In what follows we will closely follow [23]who computed the tidal torquing for a standard CDM model with gausssian spectrum.

Consider a perturbation which is growing, we can look at the evolution of shells. A given shell will contain a fixed amount of matter and shells will not cross at least until they are collapsing faster than the Hubble expansion. The gravitational torque induced on a shell, by all the surrounding matter is.

$$\tau(x) = -G \int_{x \in shell} \rho(\vec{s}) \vec{s} \times \vec{\nabla} \Phi(\vec{s}) d^3 s \tag{4.1}$$

where

$$\rho(\vec{s}) = \rho_b (1 + \delta(s))(1 + \epsilon(\vec{s})) \tag{4.2}$$

All the non–sphericity of ρ is in $\epsilon(\vec{s})$ for $\vec{s}$ much larger than the size of the texture (i.e. the other earlier textures that collapsed within this volume provide the asphericity).

Φ is the gravitational potential, which can be expanded in spherical harmonics.

$$\Phi(\vec{s}) = \sum_{l=0}^{\infty} \frac{4\pi}{2l+1} \sum_{m=-l}^{m=l} a_{lm}(s) Y_{lm}(\theta, \phi) s^l \tag{4.3}$$

where

$$a_{lm}(x) = \rho_b \int_x^{\infty} Y_{lm}(\theta, \phi)(1 + \delta(s)) \epsilon(\vec{s}) s^{-l-1} d^3 s \tag{4.4}$$

plugging (4.3)into (4.1)and using the fact that

$$\vec{x} \times \vec{\nabla}(x^l Y_{lm}(\theta,\phi)) = i x^l \vec{L} Y_{lm}(\theta,\phi) \tag{4.5}$$

where

$$\vec{L} \equiv -i(\vec{x} \times \vec{\nabla}) = \hat{x}(L_+ + L_-) + i\hat{y}(L_- - L_+)\hat{z}L_z \tag{4.6}$$

is the angular momentum operator familiar from quantum mechanics. we obtain for the z component

$$\tau_z = -iGM_{shell} \sum_{l=0}^{\infty} \frac{x^l}{2l+1} \sum_{m=-l}^{l} m a_{lm}(x) \int \epsilon(\vec{x}) Y_{lm} d\Omega \tag{4.7}$$

Let us introduce the multipole moments of the shell

$$q_{lm}(x) = \int_{shell} Y^*_{lm}(\theta,\phi) s^l \rho(\vec{s}) d^3 s = \frac{x^l}{4\pi} M_{shell} \int Y^*_{lm}(\theta,\phi)\epsilon(\vec{x}) d\Omega \tag{4.8}$$

where the final form is reached after substituting (4.2)and being left with the non-symmetric part. We can now rewrite τ_z as

$$\tau_z = -i4\pi G \sum_{l=0}^{\infty} \frac{1}{2l+1} \sum_{m=-l}^{l} m a_{lm} q^*_{lm} \tag{4.9}$$

If we retain only the quadrupole term ($l = 2$) we can compute the rms torque on a shell.

$$\begin{aligned} \langle|\vec{\tau}|\rangle &= 3\langle|\tau_z|\rangle \\ &= 3(\frac{4\pi}{5}G)^2 \sum_{m=-2}^{2} \sum_{n=-2}^{2} mn \langle a_{2m}(x) a^*_{2n}(x) q^*_{2m}(x) q_{2n}(x)\rangle \end{aligned} \tag{4.10}$$

with

$$\begin{aligned} &\langle a_{2m}(x) a^*_{2n}(x) q^*_{2m}(x) q_{2n}(x)\rangle = \\ &\frac{\rho_b^2 M^2_{shell} x^4}{(4\pi)^2} \int_x^{\infty} \frac{dr_1}{r_1} \int_x^{\infty} \frac{dr_2}{r_2} \int\int\int\int Y^*_{2m}(1) Y_{2m}(2) Y_{2m}(3) Y^*_{2n} \langle \epsilon_1\epsilon_2\epsilon_3\epsilon_4\rangle d\Omega_1 d\Omega_2 d\Omega_3 d\Omega_4 \end{aligned} \tag{4.11}$$

the final form is reached under the assumption that the 4 point function can be written as

$$\langle \epsilon_1\epsilon_2\epsilon_3\epsilon_4\rangle = \langle \epsilon_1\epsilon_2\rangle\langle \epsilon_3\epsilon_4\rangle \ + \ \langle \epsilon_1\epsilon_3\rangle \ + \ \langle \epsilon_2\epsilon_4\rangle \ + \ \langle \epsilon_1\epsilon_4\rangle\langle \epsilon_2\epsilon_3\rangle\rangle \tag{4.12}$$

which is certainly true for a random gaussian process [22], and a reasonnable approximation in our case. Then after using the definition of the power spectrum in terms of the 2 point function

$$\int\int Y^*_{2m}(1)Y_{2n}(2)\langle\epsilon_1\epsilon_2\rangle d\Omega_1 d\Omega_2 = \frac{1}{(2\pi)^3}\int d^3kP(k)\int e^{-i\vec{k}\cdot\vec{x}_1}Y^*_{2m}(1)d\Omega_1\int e^{-i\vec{k}\cdot\vec{x}_2}Y^*_{2n}(2)d\Omega_2 \tag{4.13}$$

,the expansion of a plane wave in sperical harmonics

$$e^{-i\vec{k}\cdot\vec{x}} = 4\pi\sum_{l=0}^{\infty} i^l j_l(kx)\sum_{m=-l}^{m=l} Y^*_{lm}(\theta,\phi)Y_{2m}(\theta_k, phi_k) \tag{4.14}$$

and orthogonality relations one gets

$$\tau(x) \equiv < |\tau(x)|^2 >^{\frac{1}{2}} = \quad \sqrt{30}\Big(\frac{4\pi G}{5}\Big)\Big[< a^2_{2m}(x) >< q^2_{2m}(x) - \ < a_{2m}(x)q_{2m}(x) >^2\Big]^{\frac{1}{2}} \tag{4.15}$$

where

$$< q^2_{2m}(x) >= \frac{x^4}{(4\pi)^2}VM^2_{sh}\int k^2 dkP(k,\tau)(j_2(kx))^2 \tag{4.16}$$

$$< a^2_{2m}(x) >= \frac{2\rho_b(\tau)x^{-2}}{\pi}VM^2_{sh}\int dkP(k,\tau)(j_1(kx))^2 \tag{4.17}$$

$$< a_{2m}(x)q^*_{2m}(x) >= \frac{x\rho_b(\tau)VM_{sh}}{2\pi^2}\int kdkP(k,\tau)j_1(kx)j_2(kx) \tag{4.18}$$

we find that the volume factor exactly cancels out the volume factor of the power spectrum. for the sake of brievety, we omitted the τ, τ_i dependance. Putting it back, and integrating we find

$$\frac{J(x,a,a_i)}{M_{shell}x^2} = w(x,a,a_i) = \frac{3t_{eq}}{2(2-\sqrt{2})}\int_{a_{cutoff}}^{a}\frac{da'a'\tilde{\tau}(a',x_0,a_i)}{\sqrt{1+a'}x(a,a_i)^2M_{shell}} \tag{4.19}$$

The M_{shell} factor cancels exactly the Mass factor in (4.15). $\tilde{\tau}$ is given by

$$\frac{\tilde{\tau}(x_0,a',a_i)}{M} = \frac{\tau(x(x_0,a_i,a'),a')}{M} \tag{4.20}$$

and τ is given by (4.15). $x(x_0, \tau_i, a')$ is the comoving position of a shell that was at position x_0 when the texture collapsed at conformal time a_i .

We can therefore use the texture power spectrum (3.5)to figure out the angular momentum produced by gravitational torquing. We also need the position of a shell as a functions of time. In the Texture model, Texture collapse before recombination, even in the radiation era. Collapse is modeled in the radiation era by

$$x(x_0, a, a_I) = \Big(\frac{\rho_b(a) \times (1 + \delta(a, a_i))}{\rho_b(a)}\Big)^{\frac{-1}{4}} \tag{4.21}$$

We have used the $\delta(a, a_i)$ derived by [18]. When the shell enters the matter era, we match to the spherical collapse model [22]by matching the peculiar velocity of the collapsed shell. Our integrals for the torque then runs until the turn-around time, as given by the spherical collapse model.

The angular momentum thus calculated is not directly equivalent to vorticity. It can generate a solid body-like rotation of the dark matter fluid spheroïd but it has no net vorticity. To convert this rotation into vorticity, the fluid should undergo dissipative processes or shocks. While the DM cannot undergo dissipative processes, it is still possible to convert the angular momentum from the DM shell into vorticity for the matter.

As new modes of the density fluctuations enter the horizon, the matter mode grows until it is pressure supported, and undergoes a few cycles of dissipatives acoustic oscillations. [22]It is those shock waves, oscillating in the rotating aspherical gravitational potential that transfer the angular momentum to the matter. Obtaining the efficiency of this highly non-linear phenomena at transfering vorticity will await our future developpement of a non-linear hydro code to test the details of this model. Nevertheless we will make useful approximations.

The torque is caused by a quadrupole-quadrupole interaction, whose strenght scales as $\sim a^{-6}$, and whose amplitude, proportional to P(k), goes as $\sim (1 + \frac{3}{2}a)^2$. The net result is that the torque is much more effective at early times.

This is reflected in our results. Fig 1. shows the angular velocity acquired by an object of mass $2 \times 10^{11} M_\odot$ seeded at scale factor $a_i = 0.032$ at a comoving radius of 1Mpc. Most of the angular velocity of the DM is acquired early on.

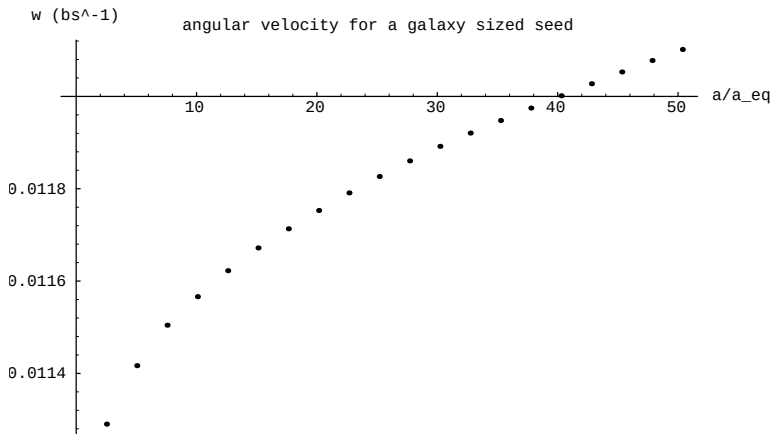

Fig. 1: angular velocity at a=50 for a texture collapsing at $0.032a_{eq}$ the units are (ls^{-1}) 1 ls = 2.79E12 seconds. The comoving radius is 1.014 Mpc and this shell contains $2 \times 10^{11} M_{\odot}$

In Fig 2. we have plotted the angular velocity attained by each shell at their own turn around time. Note that the steep distribution at low radius is made steeper because by the time the outer shells have collapsed, the center will have collapse even further, causing a spin up if angular momentum is conserved. This could possibly slow the collapse of the center.

In table 1 we have tabulated data. The angular velocity as a function of initial comoving radius follows roughly $w \sim \frac{1}{x^{\frac{5}{3}}}$ and $w \sim \frac{1}{a_i^{\frac{5}{3}}}$ we can compute the magnetic field for different size textures from (2.1). After the radiation era, $w \sim a^{\frac{1}{30}}$ so we can take w approximatively constant. As noted in the appendix we need the angular velocity of those

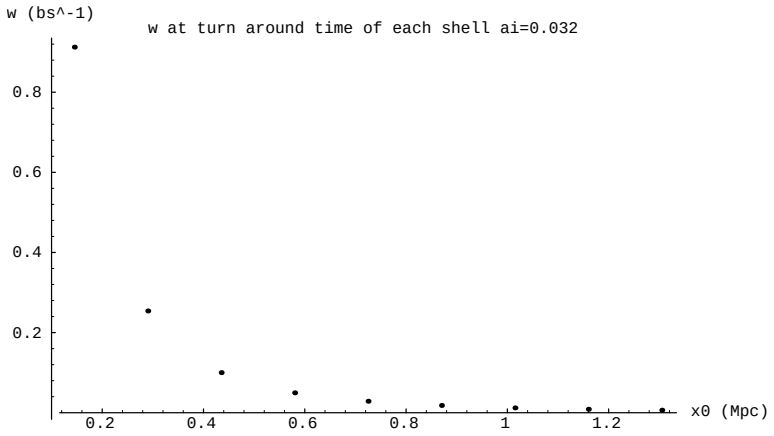

Fig. 2: angular velocity at the turn-around time as a function of the unperturbed comoving radius for a texture collapsing at $0.032a_{eq}$. Note that each x_{ta} is reached at a different time. the units are (ls^{-1}) 1 $bs = 2.79 \times 10^{12}$ seconds. A comoving radius of contains $2 \times 10^{11} M_{\odot} (\frac{x}{1Mpc})^3$

shells that reached their turn around point before recombination($a \sim 5$). This gives that for a typical galaxy-sized object ($a_i = 0.048$,$x_0 = 1Mpc$,$z_f = 116$, $\Rightarrow M_{gal} = 10^{12} M_{\odot}$) only regions inside a comoving radius of 0.2 Mpc have reached their turn-around radius. For those radii we obtain $\omega \sim 0.3ls^{-1}$. To compute a magnetic field we need to know how efficiently has the DM transfered it's angular momentum to the matter component. Let us get an upper limit to the possible magnetic field. Assuming 100% conversion, the matter acquires an angular velocity of w. We use (2.1)to get $B \sim 2 \times 10^{-17}$ gauss. At that ealy epoch, the density of the proto galaxy is actually bigger than that of the final

object. Upon complete collapse to the density of a galaxy, this field will be multiplied by $(\frac{\rho_{collapse}}{rho_{galaxy}})^{2/3} \sim 3 \times 10^{-2}$ So textures can yield at most a seed field of 6×10^{-19} gauss for galaxy sized perturbations.

Our galaxy has a rotational velocity of $w \sim 0.0005$ in our units. The generated angular velocity for a galaxy-sized object was $\omega \sim 0.3ls^{-1}$, at recombination, which we have to multiply by the windup factor, 3×10^{-2}, to yield 10^{-3}. This number has to be multiplied by the efficiency factor of conversion of DM angular momentum into matter vorticity. This shows that the required conversion factor cannot be as high as 100% .but has to be less about 10% . Under that assumption, the angular momentum of galaxy-sized objects produced by the texture scenario is adequate.

5. Conclusion

In the early universe, the texture model can produces sizable angular momentum. A similar analysys using the power spectrum of CDM has been peeformed by Ryden [23]. For both models the values are consistent with our own galaxy.

In the texture model the early formation of angular momentum yields to formation of a magnetic field. On the other hand for the CDM model no magnetic field can be generated by that angular momentum because all of it was acquired after recombination. Our Scenario can only produce magnetic field in Clusters if a hiearchical model of cluster formation is adopted. This model only produced magnetic field in Galaxy sized objects and none in the interstellar medium other than that carried by the gas ejected from proto-objects.

The upper limit we compute for the magnetic field falls short of the modern estimates of the required seed field. Although the texture model fares better in this problem than the standard CDM model, it does not pass this test. Magnetic field creation through early AGN is a better possibility in the texture model than in CDM because the structures form earlier.

The scenario we have developped shows us that any model that yields non-baryonic growing density perturbations by the epoch of recombination can produce magnetic fields.

6. Acknowledgements

I would like to thank David Spergel, Russel Kulsrud, Jim Peebles and Bharat Ratra for helpful discussions and references. I also want to thank to Neil Turok for suggesting to investigate this topic.

Table 1			
a_i	x_0	a/a_{eq}	w (ls^{-1})
0.003	0.0139606	0.134108	20.6876
0.003	0.0698029	1.11764	3.46906
0.003	0.139606	6	1.25885
0.004	0.0184639	0.18984	15.9377
0.004	0.0923195	1.58212	2.33627
0.004	0.184639	8	0.773242
0.006	0.0274655	0.31313	10.6319
0.006	0.137327	2.60968	1.28811
0.006	0.274655	12	0.334348
0.008	0.0364617	0.450027	7.92929
0.008	0.182309	3.75069	0.789084
0.008	0.364617	16	0.167428
0.012	0.0546771	0.762122	4.83116
0.012	0.273386	6.35207	0.33716
0.012	0.546771	24	0.0595082
0.016	0.0728387	1.1155	3.26369
0.016	0.364193	9.2977	0.167547
0.016	0.728387	32	0.0288167
0.024	0.109059	1.93168	1.76581
0.024	0.545294	0.805078	0.057496
0.024	1.09059	48	0.0101015
0.032	0.144989	2.87665	0.912561
0.032	0.724945	1.19898	0.0274236
0.032	1.44989	64	0.00471943
0.048	0.216372	5.12164	0.287895
0.048	1.08186	42.6972	0.0102267
0.048	2.16372	96	0.00157769

In this table we list the angular velocity acquired by the DM shell up to the point where the DM shells turns around. This value is calculated at the epoch of the turn around of each shell. The scale factor at that turn around time is given in column 3. These quantities are given for a range of initial texture collapse and initial co-moving radius.

Table 1			
a_i	x_0	a/a_{eq}	w (ls^{-1})
0.064	0.28702	7.80306	0.129639
0.064	1.4351	65.0556	0.00479661
0.064	2.8702	128	0.000734812
0.096	0.426246	14.3865	0.0423705
0.096	2.13123	119.955	0.00165626
0.096	4.26246	192	0.000283749
0.128	0.562777	22.5143	0.0190206
0.128	2.81388	187.74	0.00081579
0.128	5.62777	256	0.00015816
0.172	0.746374	36.1093	0.00949166
0.172	3.73187	301.128	0.000447707
0.172	7.46374	344	9.5687e-05
0.256	1.08455	69.5543	0.00365715
0.256	5.42276	512	0.000228605
0.256	10.8455	512	5.06313e-05
0.384	1.57217	138.656	0.0014671
0.384	7.86085	768	9.83743e-05
0.384	715.7217	768	2.08143e-05
0.512	2.03084	228.674	0.000952099
0.512	10.1542	1024	5.26307e-05
0.512	20.3084	1024	1.04759e-05
0.768	2.87671	467.535	0.000655441
0.768	14.3835	1536	2.13841e-05
0.768	28.7671	1536	3.3304e-06
1.024	3.64583	779.061	0.000399587
1.024	18.2291	2048	1.0869e-05
1.024	36.4583	2048	3.00253e-07
1.536	5.01273	1598.52	0.000185055
1.536	25.0637	3072	3.60041e-06
1.536	50.1273	3072	0
2.048	6.21222	2655.68	0.000103789
2.048	31.0611	4096	9.4301e-07
2.048	62.1222	4096	0
2.99	8.12198	5168.26	4.47294e-05
2.99	40.6099	5980	0
2.99	81.2198	5980	0

7. Appendix 1

Here we will derive the equation for the Harrison mechanism.

$$\frac{D_j}{D\tau} = \frac{d}{dt} + \vec{v}_j \cdot \vec{\nabla} = \frac{\partial}{\partial t} + \vec{V}_j \cdot \vec{\nabla} \tag{7.1}$$

is the standard convective derivative where $\frac{d}{dt}$ follows the expansion and $V_j = \dot{R}\vec{x} + R\dot{x}$. $\dot{R}\vec{x}$ is the hubble flow with the other term being the the peculiar velocity. In an expanding Universe it must be replaced by

$$\frac{1}{R}\frac{D}{D\tau}\big(R\vec{v}\big) = \frac{\partial \vec{v}}{\partial t} + \frac{\dot{R}}{R}\vec{v} + \frac{1}{R}\big(\vec{V}\cdot\vec{\nabla}\vec{v}\big) \tag{7.2}$$

where we often replace $\frac{\dot{R}}{R}$= H , which is the hubble expansion rate.

The equation for the electron motion is

$$\frac{\rho_e}{R}\frac{D}{D\tau}\big(R\vec{v}_e\big) = -\frac{en_e}{c}\big(\vec{E} + \frac{1}{c}\vec{V}_e \times \vec{B} - \frac{\vec{j}}{\sigma}\big) + \frac{4}{3}\rho_\gamma n_e c\sigma_{T_e}(\vec{v}_\gamma - \vec{v}_e) - \frac{\nabla p}{R} - \frac{\rho_e \nabla\phi}{R} \tag{7.3}$$

the ion equation is

$$\frac{\rho_e}{R}\frac{D}{D\tau}\big(R\vec{v}_p\big) = +\frac{en_p}{c}\big(\vec{E} + \frac{1}{c}\vec{V}_p \times \vec{B} - \frac{\vec{j}}{\sigma}\big) + \frac{4}{3}\rho_\gamma n_e c\sigma_{T_p}(\vec{v}_\gamma - \vec{v}_e) - \frac{\nabla p}{R} - \frac{\rho_p \nabla\phi}{R} \tag{7.4}$$

and the photon equation is

$$(\rho_\gamma + \frac{1}{c^2}p_\gamma)\frac{1}{R}\frac{D}{D\tau}\big(R\vec{v}_\gamma\big) = -\frac{1}{c^2}\vec{V}_\gamma\frac{d}{dt}p_\gamma - (\rho_\gamma + \frac{1}{c^2}p_\gamma)\nabla\phi - \frac{4}{3}\rho_\gamma n_e c\sigma_{T_e}(\vec{v}_\gamma - \vec{v}_e) - \frac{4}{3}\rho_\gamma n_p c\sigma_{T_p}(\vec{v}_\gamma - \vec{v}_p) \tag{7.5}$$

$$+\frac{4}{3}\frac{\rho_\gamma c}{5n\sigma}\nabla^2\vec{v}_\gamma \tag{7.6}$$

We drop the last term, because the conductivity is very large at that epoch. If we use the continuity equation

$$\vec{\nabla}\cdot\vec{V} = \frac{-1}{\big(\rho_\gamma + \frac{1}{c^2}p_\gamma\big)}\frac{d\rho_\gamma}{dt} \tag{7.7}$$

and $p_\gamma = \frac{1}{3}\rho_\gamma c^2$ and $\vec{\nabla}\cdot\vec{V}_\gamma = 3H + \vec{\nabla}\cdot\vec{v}$

we get

$$\rho_\gamma\frac{D}{D\tau}\vec{v}_\gamma = -\frac{1}{3}\rho_\gamma\vec{V}_\gamma(\vec{\nabla}\cdot\vec{v}_\gamma) - \rho_\gamma\vec{\nabla}\phi - c\sigma_{T_e}\rho_\gamma n_e(\vec{v}_\gamma - \vec{v}_e) - c\sigma_{T_p}\rho_\gamma n_p(\vec{v}_\gamma - \vec{v}_p) \tag{7.8}$$

Note that we will be taking the curl of (7.3)(7.4)and (7.8)so that the pressure and gravitational term will go away. A short calculation of $\vec{\nabla}\times$(7.4)yields

$$\frac{1}{R^2}\frac{D}{D\tau}(R^2\vec{\zeta})+\vec{\zeta}(\vec{\nabla}\cdot\vec{v})-(\vec{\zeta}\cdot\vec{\nabla})\vec{v}=-\frac{n_p e}{\rho_p c}\frac{1}{R^2}\frac{D}{D\tau}\big(R^2\vec{B}\big)+\frac{c}{4\pi\sigma_{cond}}\left(\frac{1}{\mu}\vec{\nabla}^2\vec{B}-\frac{\epsilon}{c^2}\ddot{\vec{B}}\right)-\frac{4}{3}\frac{\rho_\gamma}{\rho_p}n_p c\sigma_{T_p}(\vec{\zeta}_\gamma-\vec{\zeta}_p) \tag{7.9}$$

where to find the RHS we assumed that $\vec{B}\cdot\nabla\vec{V}=H\vec{B}$ which is only exactly true at $\theta=\frac{\pi}{2}$. The conductivity σ being very high, we can drop the wave equation term in $\vec{B}$. With

$$\alpha_p=\frac{n_p e}{\rho_i c}=\frac{e}{m_p c} \tag{7.10}$$

we can finally write $\nabla\times$(7.4)as

$$\frac{1}{R}\frac{D}{D\tau}\big[R^2\big(\vec{\zeta}_p+\alpha_p\vec{B}\big)\big]=-\frac{4}{3}\frac{\rho_\gamma}{m_p}c\sigma_{T_e}(\vec{\zeta}_\gamma-\vec{\zeta}_e) \tag{7.11}$$

similarly $\nabla\times$(7.3)yields

$$\frac{1}{R}\frac{D}{D\tau}\big[R^2\big(\vec{\zeta}_e-\alpha_e\vec{B}\big)\big]=\frac{4}{3}\frac{\rho_\gamma c\sigma_{T_p}}{m_e}\big(\vec{\zeta}_\gamma-\vec{\zeta}_e\big) \tag{7.12}$$

Right away we notice that the electron dynamics is much more affected by the photon drag due to the smaller electron mass on the denominator of the RHS of (7.12). Also notice that in (7.11)and (7.12)$\sigma_{T_e}/m_p=\sigma_{T_p}/m_p$. Taking the curl of (7.8)yields

$$\rho_\gamma\frac{1}{R}\frac{D}{Dt}\big(R\vec{\zeta}_\gamma\big)=-n_e c\sigma_{T_e}\rho_{gamma}\big(2\vec{\zeta}_\gamma-\vec{\zeta}_e-\vec{\zeta}_p\big) \tag{7.13}$$

where we have assumed $\vec{\nabla}\cdot\vec{v}$ is small .

((7.12)+ (7.11)) yields

$$\frac{1}{R}\frac{D}{D\tau}\big[R^2\big(\vec{\zeta}_p+\vec{\zeta}_p\big)\big]=\frac{1}{R}\frac{D}{D\tau}\big[R^2\big(\alpha_e\vec{B}\big)\big] \tag{7.14}$$

We have used $\alpha_e\gg\alpha_p$. Since the proton will spin down faster than the electron, the proton vorticity will be small. Integrating (7.14)yields the wanted result (2.1).

This was derived under the assumption that the matter background is spinning down faster from having the same initial angular velocity as the radiation. In the original Harrison mechanism, the vortices were primordial and the radiation had the same initial velocity as the matter. The evolution was different because for the radiation (and the

electrons tied to it by the strong Thompson cross section) $L = \rho V r^2 \omega \sim a^{-4} a^3 a^2 \omega =$ *constant* so $\omega_\gamma \sim a^{-1}$ where a is the scale factor, whereas for the matter $w \sim a^{-2}$.

In our model the angular velocity will be provided by angular torquing (+ dissipation). We have to require that the angular momentum gained by the matter has had time to spin down. For angular velocity acquired by gravitational torquing (+ dissipation) , most of the angular momentum of the matter should be acquired by the time the dark matter shell has reached it's turn around radius. Before recombination the photon mean free path $l_\gamma = \frac{1}{n_e \sigma_T}$ is $6 \times 10^{-5} Mpc \Omega_0^{-1} h_{50}^{-1} (\frac{1100}{1+z})^3$ so that density perturbation of the radiation by textures don't have time to diffuse out of their creation region before recombination and they will acquire angular velocity to due gravitational torquing+dissipation just as the matter did. So at a given shell radius, the angular momentum growth must peak before recombination ($a \sim 5$) in order to have a sizable magnetic by the Harrison mechanism.

References

[1] J.S., Hall Science **109** (1949) 166

[2] W.A., Hiltner Science **109** (1949) 165

[3] A.A. Ruzmaikin "Galactic and Intergalactic Magnetic fields", Kluwer Academic Publisher (1990) p. 88

[4] N. Turok, Phys. Rev. Lett. **63** (1989) 2625

[5] H.K. Moffatt Magnetic Field generation in electrically conducting fluids (Cambridge U. Press, 1978)

[6] F. Krause and K.-H. Rädler, Mean Field MHD and Dynamo Theory,1980 Pergamon Press

[7] E.N. Parker, Cosmical Magnetic Fields, 1979 Clarendon Press- Oxford

[8] Ed. R. Beck, , P.P. Kronberg and R. Wielebinski , Galactic and Intergalactic Magnetic Fields, IAU Symposium no. 140, 1989 Kluwer Academic Publishing

[9] R.M. Kuldrud, IAU Symposium no. 140, 1989 Kluwer Academic Publishing

[10] R. M. Kulsrud and S. W. Anderson , ApJ **396** (1992) 606

[11] E.N. Parker , ApJ **401** (1992) 137

[12] B. Ratra, Ap. J **391** (1992) L1

[13] Daly, R, Loeb, A. Ap. J. **364**(1990) 951

[14] E.R. Harrison, Mon. Not. R. astr. Soc. **147** (1970) 279

[15] E.R. HArrison, MNRAS **165** (1973) 185

[16] Kibble T.W.B., J. Phys. **A9** (1976) 1387

[17] N. Turok, Princeton preprint PUP-TH-1230 to appear in "The Birth and Evolution of Our Universe", proceedings of Nobel Symposium, Sweden

[18] A. K. Gooding, Princeton University PhD thesis (1991)

[19] Derrick 1964

[20] Hobard 1963

[21] Ue-Li Pen,D.N. Spergel and N.Turok, PUP-TH-1375 (1993)

[22] P.J.E.P. Peebles Physical Cosmology, 1980

[23] B. S. Ryden PhD thesis , Princeton 1987